ICARUS 113, 188–199 (1995)

The Coefficient of Restitution of Ice Particles in Glancing Collisions: Experimental Results for Unfrosted Surfaces

KIMBERLEY D. SUPULVER

Board of Studies in Astronomy and Astrophysics, University of California, Santa Cruz, California 95064
E-mail: supulver@lick.ucsc.edu

FRANK G. BRIDGES

Board of Studies in Physics, University of California, Santa Cruz, California 95064

AND

D. N. C. LIN

Board of Studies in Astronomy and Astrophysics, University of California, Santa Cruz, California 95064

Received March 12, 1993; revised September 19, 1994

Both Saturn's rings and planetesimal disks are made up of particles in Keplerian orbits. Inelastic collisions between these particles regulate their dynamical evolution and possible aggregation. We present an experiment to simulate glancing collisions in Saturn's rings and in planetesimal disks and thus measure contributions to the energy loss for both normal and tangential velocity components. In this experiment, a spherical iceball mounted on a long-period, two dimensional pendulum is made to impact a flat ice surface in a low-temperature environment. This paper describes the experimental apparatus in detail and presents results for smooth unfrosted surfaces. The energy loss for tangential motion is surprisingly low, indicating that very little friction is present at low impact speeds for relatively smooth ice surfaces and temperatures near 100 K. We have also investigated room-temperature collisions of a rubber ball on a rough surface to understand the energy loss in situations where the tangential friction force is not small. In this analogous case, the energy loss is maximum for impact angles in the range 45°–60°. © 1995 Academic Press, Inc.

I. INTRODUCTION

Planetary rings and planetesimal disks are composed of particles which revolve around the central body on nearly circular Keplerian orbits. The collisional properties of such particles are critical in determining their dynamical properties (Goldreich and Tremaine 1982). For example, the velocity dispersion in a planetary ring is regulated by a balance between energy transfer from the systematic shearing motion to random dispersive motion and the energy dissipated during inelastic collisions (Goldreich and Tremaine 1978, Stewart *et al.* 1984, Shu and Stewart 1985). The equilibrium configuration constrains the thickness and stability of planetary rings (Brahic 1977, Lin and Bodenheimer 1981, Ward 1981, Lukkari 1981, Hämeen-Antilla 1982, Araki and Tremaine 1986). In planetesimal disks, collisions not only control the dynamical properties of the disk particles but also determine the rate of coagulation among planetesimals (Palmer *et al.* 1993, Aarseth *et al.* 1993) under the assumption of a nonzero sticking probability.

Quantitatively, the amount of energy dissipated during each collision can be expressed in terms of the coefficient of restitution, ε, which is defined as the ratio of postcollision relative speed to precollision relative speed: $\varepsilon = v_{out}/v_{in}$. Thus, the quantity $(1 - \varepsilon^2)$ is a measure of the energy lost in the collision; $\varepsilon = 1.0$ represents a totally elastic collision, while $\varepsilon = 0.0$ represents a totally inelastic collision (i.e., the two particles stick together).

Bridges *et al.* (1984) and Hatzes *et al.* (1988) designed and built an apparatus to determine the coefficient of restitution of water ice particles in normal (radial) collisions in order to understand the dynamical processes occurring in the rings of Saturn. The apparatus, a disk pendulum similar to that pictured in Fig. 1, was designed to impact a spherical iceball in the direction normal to a stationary flat ice surface (an ice brick); it was not possible to investigate glancing collisions with this apparatus. However, glancing collisions commonly occur and can have important effects on the kinematic spin properties of the particles (Araki 1988) and the nonlinear dissipation of density waves excited by satellites (Shu *et al.* 1985). In planetesimal disks, they also determine the balance

0019-1035/95 $6.00

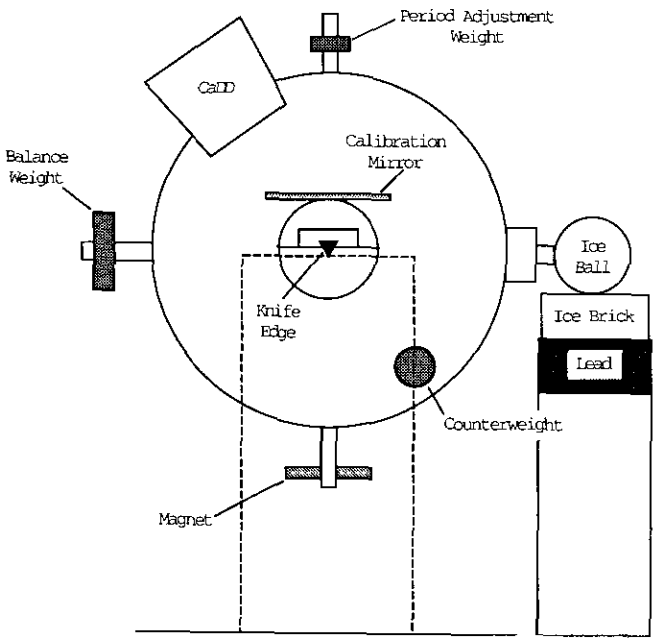

FIG. 1. Side view of the disk pendulum used by Bridges *et al.* (1984) and Hatzes *et al.* (1988) to investigate the behavior of ε as a function of normal impact velocity. The ice brick is secured to a lead brick for stability. The pendulum oscillates freely on the agate knife edges, moving the iceball up and down in the direction normal to the ice brick surface, allowing the iceball to collide with the brick.

between the spin energy and orbital energy of the planetesimals (Lin *et al.* 1993).

In this paper we present results for the coefficient of restitution in glancing incidence collisions for relative speeds in the range 0.02 to 1 cm sec^{-1}. This experiment is carried out with some modifications of our original apparatus such that the motion of the iceball now occurs in two dimensions. The motion of the iceball is still restricted, however, in the sense that no transfer of energy into spin degrees of freedom is permitted. A brief description of the apparatus is given in Section II.

We carry out our experiments with iceballs (spheres of frozen distilled water, 2.5 cm in radius) at temperatures near 100 K because centimeter- to meter-sized ice particles are the main constituent bodies in Saturn's rings, and the estimated ring temperatures are $\simeq$100 K (Cuzzi *et al.* 1984). In the context of planetary formation, the temperature in the outer regions of the solar nebula is expected to have been below the ice condensation temperature (Lin and Papaloizou 1980, 1985); therefore, it is likely that particles in these regions had a surface coating of ice. Centimeter-sized particles with a density of 1 g cm^{-3} in the outer nebula (at a radius of $\simeq$30 AU) would have estimated relative velocities of a few cm sec^{-1} (Völk *et al.* 1980, Mizuno *et al.* 1988). Consequently, values of ε for the highest velocities we attain with our apparatus are also applicable to centimeter-sized particles in models of the outer solar nebula. The experimental data are summarized in Section III.

It has been suggested that the presence of surface frost may be needed for planetesimal coagulation (Bridges *et al.* 1994). In the present experiments with frost-free surfaces, we have observed no sticking contacts in several hundred collisions (sticking force <1 dyne). These results strengthen our conjecture that smooth, frost-free surfaces do not adhere and that particles with frost-free surfaces will not form stable aggregates. Thus, experimental investigations of iceball collisions provide useful information about particle aggregation and dynamics in both planetary rings and planetesimal disks. The implications of our results are summarized in Section IV.

II. THE APPARATUS

The apparatus is a two-dimensional pendulum, shown in side view in Fig. 2, which allows an iceball to impact a stationary ice brick at various angles and velocities. The double pendulum consists of a disk pendulum (Fig. 1), oscillating on agate knife edges, supported inside a torsion pendulum which oscillates by twisting about a wire suspended from a point at the top of a cryostat. These two types of support were chosen because the resulting energy loss in rotational motion is extremely low. The kinetic energy in these experiments is very small (10^{-2} to 10^{3} ergs); thus, the total frictional forces must be very small so that the pendulum oscillates freely over a time of $\simeq$20 sec (one period is typically 10 sec) with minimal energy loss. For the lower speeds, the friction force must be much less than 1 dyne. The support system must also be rigid against shear motion at the instant of contact; the agate bearings are particularly good in this regard, because the reaction impulse force is vertical. For the torsion pendulum, we had to add shear bearings above and below the suspended cage (which holds the disk pendulum) to eliminate lateral motions. These bearings provide no support and supply only momentary horizontal thrust for the short time of the collision. We found that tiny bearings, formed by a 1-mm rod through a thin piece of brass, provided the required sideways thrust, with little reduction in the quality factor (Q) when the bearings were carefully aligned. The bearings had to be adjustable, because slight distortions of the cryostat, caused by thermal contraction during cool-down, can cause misalignment. The requirement of rigid, very low friction bearings capable of supporting 100 to 1000 g, operating at low temperatures, has precluded mounting the iceball on bearings.

In an experimental run, the cryostat is cooled to approximately 100 K using liquid nitrogen; the ambient atmosphere is nitrogen gas at atmospheric pressure to achieve thermal contact between the pendulum, ice particles, and

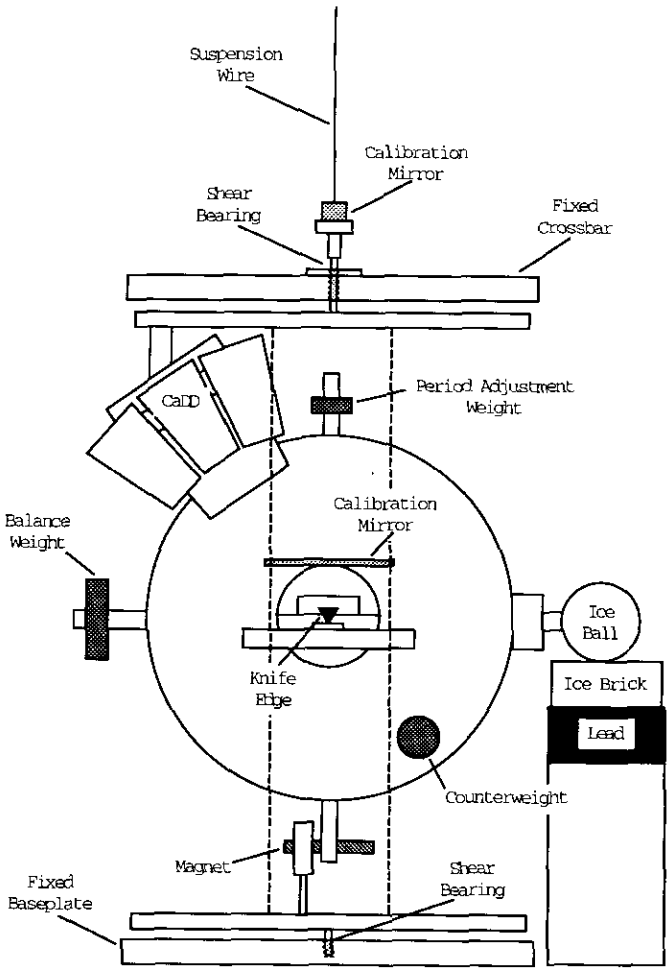

FIG. 2. Side view of the modified pendulum apparatus used in this current work. The disk pendulum operates as in Fig. 1; the additional degree of freedom to allow for glancing collisions is provided by a torsion pendulum, suspended from a wire, within which the disk pendulum is mounted. The torsion pendulum oscillates freely about the suspension wire, allowing the iceball to move left and right in the direction parallel to the ice brick surface at the same time as the disk pendulum oscillates.

the cold section of the cryostat. Earlier experiments showed that there was no significant change in ε for different pressures ranging from one atmosphere down to 10^{-5} torr (Hatzes *et al.* 1988).

The position of the iceball is measured with capacitive displacement devices (CaDDs). One CaDD, depicted in Fig. 2, detects the position of the iceball in the direction normal to the ice brick surface; an analogous CaDD (not pictured in Fig. 2) detects the position of the iceball in the direction parallel to the ice brick surface. Hatzes *et al.* (1988) provide a detailed description of the operation of the CaDD system.

The apparatus is computer-controlled; the iceball is lifted to a given position above the ice brick, held in place, and then released to impact the brick. Both the disk pendulum and the torsion pendulum are moved magnetically by controlling the current in a coil surrounding a cylindrical magnet. This mechanism is shown in Fig. 2 for the disk pendulum (an analogous coil and magnet, not shown in Fig. 2, control the torsion pendulum). As the iceball impacts the ice brick, the time-varying voltage output from the CaDDs is recorded by a computer and converted into position coordinates using voltage vs position calibration factors which are determined at the beginning of each experimental run. In this manner, a position vs time track is established for a given collision, the precollision and postcollision velocities are measured from the slope of this track (over a time within 0.5 s of the collision), and ε and the impact angle θ are calculated. The total impact velocity v as well as the components normal and tangential to the ice brick surface can be determined. In this work, θ is defined from the horizontal; thus, a 90° collision is a normal (radial) collision, while a 0° collision is a tangential collision. Uncertainties in v and ε can range up to a few percent, resulting in error bars just slightly larger than the symbols in Figs. 3–5 and 7–10 at high speeds ($v > 0.2$ cm sec^{-1}) and up to $\pm 5\%$ at the lowest speeds. Data can be taken with different time resolutions; the data presented in this paper have a time resolution of approximately 1–2 msec.

We have measured ε at a given impact speed and angle for both possible directions of tangential impact (the torsion pendulum can move the iceball either to the left or to the right of its equilibrium point). From these measurements, we have determined that there is no systematic difference in ε for the two impact directions; the apparatus is "symmetric" in this sense.

There is, inevitably, a small degree of coupling between the two penduli (the disk pendulum and the torsion pendulum). However, the coupling is extremely small, and is not enough to affect the results when the two periods are not equal. (Typically, the periods differ by ~10%.) We measured this transfer of energy by starting with both penduli stationary, then displacing one pendulum a fixed distance and releasing it. The second pendulum responded with a tiny oscillation. The periods of the disk and torsion penduli were 10.65 and 11.25 sec, respectively. The kinetic energy of oscillation of one pendulum is $E = M_{\text{eff}}(\omega x)^2/2$, where M_{eff} is the effective mass of the pendulum for a given moment of inertia, ω is the frequency of oscillation, and x is the displacement of the pendulum. Coupling of energy from the disk pendulum radial motion (E_n) to torsion pendulum tangential motion (E_t) ranged from $\simeq 10^{-4}$ to $10^{-3}\%$ (i.e., less than 0.001% of the initial kinetic energy of the disk pendulum is transferred into motion of an initially stationary free torsion pendulum). Coupling from the torsion pendulum motion to disk pendulum motion (E_n/E_t) was consistently $\simeq 10^{-3}\%$. The difference in the magnitude of the coupling is due to the

different effective masses of the two penduli; $M_{\mathrm{eff},n}$ is approximately 1/3 $M_{\mathrm{eff},t}$.

Because the effective masses of the two penduli are different, we calculate ε weighted by the masses of the penduli according to the formula

$$\varepsilon = (M_{\mathrm{eff},n}v_{\mathrm{out},n}^2 + M_{\mathrm{eff},t}v_{\mathrm{out},t}^2)/(M_{\mathrm{eff},n}v_{in,n}^2 + M_{\mathrm{eff},t}v_{in,t}^2). \quad (1)$$

This new definition of ε has the largest effect at intermediate impact angles, where $v_n \simeq v_t$. At extreme angles, ε is dominated by either its radial (for near-normal collisions) or tangential (for near-grazing collisions) component, and the weighting has little effect.

During a collision, there can be a transfer of energy from horizontal to vertical motion (or vice versa) if one or both of the following situations obtains: (1) the contact point is not directly below the center of the iceball and/or (2) the flat ice brick surface is not level. We have investigated these types of energy transfer at room temperature, using a rubber ball in place of the iceball and an aluminum brick in place of the ice brick, and we have shown that they are easy to eliminate for a smooth contact surface. The molded iceball is very well centered on the support structure, so the first possibility is not important. One can verify that the flat surface is level by performing a few radial collisions with the horizontal pendulum free to oscillate but initially stationary. If the surface is not level, the horizontal pendulum will move consistently upon collision in a direction determined by the slope of the flat surface. In forming the ice brick, a thin layer of water is allowed to freeze on the surface of the solid ice brick after the brick is positioned correctly in the apparatus at a temperature just below 0°C; thus, the surface of the brick must be macroscopically level. If the ice surfaces are locally rough, there can be some random energy transfer between the two motions. This will be discussed in more detail below.

Small amounts of energy can also be transferred upon impact to a higher-frequency (~2 Hz) "rocking" mode of oscillation of the entire pendulum apparatus about an axis roughly parallel to the axis of the disk pendulum. The pendulum cage tilts forward and backward, in the direction of the oscillation of the disk pendulum. This motion is visible as a rapid, low-amplitude oscillation in the vertical position of the ice particle. We can damp this mode quite effectively, using the shear bearings described previously, so that those rapid oscillations are no longer observed.

Another effect which contributes to uncertainties in the measurement of ε is the positioning of the ice brick. The ambient temperature in the dewar slowly increases with time (~10 K/hr at our low operating temperatures), and liquid nitrogen must be periodically added to keep the temperature low. Because of these temperature changes, the vertical position of the brick must be periodically adjusted over the course of a run as the apparatus expands and contracts slightly in response to changes in temperature. These adjustments are typically performed after 5–10 consecutive collisions, depending upon the actual temperature increase over the time of those collisions; the brick is moved ~100 μm at each adjustment. At the lower impact speeds (<0.2 cm sec^{-1}), small errors in the positioning of the brick (ideally, the brick is to be placed exactly at the equilibrium position of the disk pendulum) can result in small shifts in ε_n for a given v_n. We have noticed this effect in radial iceball collisions as well as in radial rubber ball collisions. For the case of iceball collisions, however, uncertainties in ε due to errors in brick positioning are much smaller than the scatter due to collisions with an uncompacted ice brick surface.

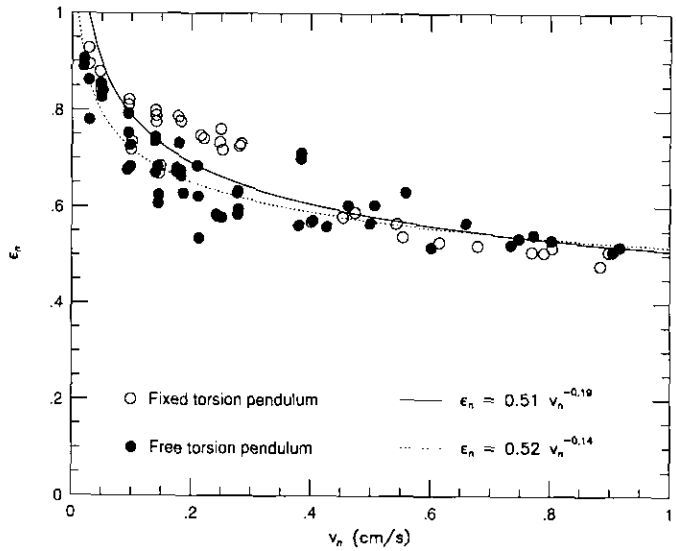

FIG. 3. Radial collisions, smooth ice surfaces. Two sets of data are presented; each symbol represents a single collision. Open circles correspond to radial impacts with the torsion pendulum fixed and unable to oscillate. Solid circles correspond to radial impacts with the torsion pendulum free to oscillate. The solid (dotted) line is a least-squares fit to the data for the case of a fixed (free) torsion pendulum.

III. DATA

A. Radial Collisions

In order to provide a direct comparison to previously published (purely radial) data (Bridges *et al.* 1984, Hatzes *et al.* 1988), we performed a series of iceball runs in which all collisions were normal. The results are shown in Fig. 3. The two different sets of data correspond to two different configurations of the double pendulum, one in which the torsion pendulum is fixed and unable to oscillate and one in which the torsion pendulum is suspended and able to

oscillate freely. At the lower speeds, significant scatter is evident in the data; this scatter is dominated by effects due to the roughness of the ice surfaces. At high speeds, the two sets of data are consistent, within the scatter. At speeds approaching 1 cm sec^{-1}, ε_n approaches 0.5. A least-squares fit to the data in Fig. 3 yields the following power laws for the cases of a fixed and free torsion pendulum, respectively:

$$\varepsilon_n = (0.51 \pm 0.01) v_n^{-0.19 \pm 0.01}, \quad (2)$$

$$\varepsilon_n = (0.52 \pm 0.01) v_n^{-0.14 \pm 0.01}. \quad (3)$$

Equation (2) for the fixed torsion pendulum is very close to that obtained by Hatzes *et al.* for compacted frost ($\varepsilon_n = 0.48 v_n^{-0.20}$) at temperatures near 120 K. Most of the new data were taken at ≈100 K. The data for the free torsion pendulum (Eq. (3)) have a weaker velocity dependence; the major effect is a smaller value of ε_n at low velocities.

In the ice particle collisions, scatter due to the contact surfaces themselves is larger than scatter due to errors in brick positioning, as long as those errors are kept within reasonable bounds (<100 μm). The brick surface is not completely smooth, and after collisions a white area on the initially clear ice surface shows the area of contact. This indicates that some fracturing has occurred, leaving a number of fine ice particles (chips) on the surface which are similar to frost. In a collision, energy is lost in fracturing the main ice surfaces, fracturing the small ice chips formed in earlier collisions, and moving the ice chips. Hatzes *et al.* (1988) found that it takes several (5–10) successive collisions at the same point of contact to compact two ice surfaces which initially were finely fractured or were covered with frost particles. For the case of a free torsion pendulum, the contact region is continually changing; we hypothesize that the surface never reaches the compacted form obtained when the horizontal motion is suppressed, and as a result, ε_n is lower and shows significant scatter.

At lower impact speeds ($v_n < 0.2$ cm sec^{-1}), the scatter in ε_n is larger, and we often observe significant motion of the torsion pendulum when the iceball impacts the ice brick when the torsion pendulum is free to oscillate. During the test runs with the smooth rubber ball described below, we observed no such horizontal motion of the ball following a radial impact even at these low impact speeds. We attribute the horizontal motion for this range of speeds to irregularities in the ice surfaces themselves; the surface is not locally level either as a result of the roughness in the original surface or due to ice chips made in higher speed collisions. An iceball impacting the brick at a very low speed may not have enough energy to dislodge or break off small protrusions nor enough energy to fracture the larger ice chips. Kinetic energy of vertical motion can thus be transferred into horizontal motion, resulting in a reduced ε_n for some of the lower-speed normal collisions. The scatter in ε_n vs v_n is even larger for the glancing collisions discussed in subsection B below, since the torsion pendulum can then sample an even greater area of the ice brick surface.

We have carried out the same experiment using a hard rubber ball in place of the iceball and a flat aluminum surface in place of the ice brick. ε_n is ≈3% lower at the higher speeds when the torsion pendulum is free to oscillate (see Fig. 4). (At the lower speeds, the scatter in the data is dominated by small errors in brick positioning.) This 3% energy loss, if it were to go into horizontal oscillation of the torsion pendulum, would result in oscillations of amplitude ~0.1 cm for the higher speeds, which would be easily observable; however, this magnitude of horizontal motion was not observed. Our measurements of the amount of coupling between the two penduli, discussed above, showed that <0.001% of the initial vertical kinetic energy would be transferred into horizontal motion—a negligible effect. Therefore, the energy must be lost through some other channel.

The extra energy loss, over and above coupling effects, is most likely due to small motions of the pendulum apparatus which cannot be completely damped out. We can damp the "rocking" mode of oscillation quite well, as discussed in the previous section, but residual small motions remain. This small systematic decrease in ε_n cer-

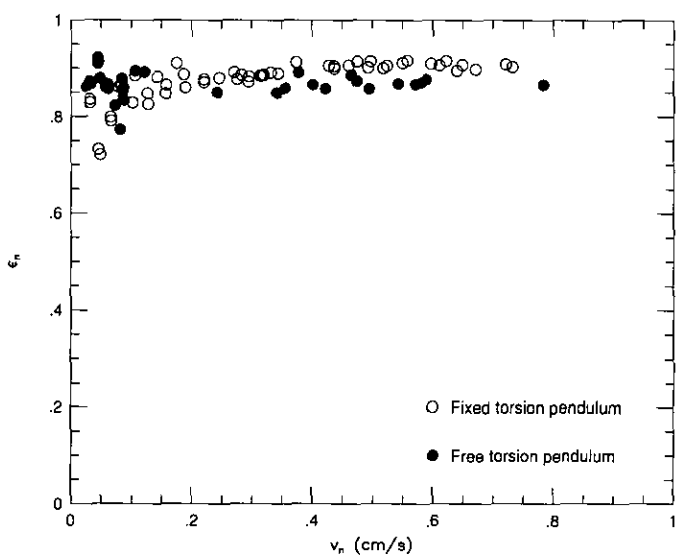

FIG. 4. Radial collisions. These data were taken with a rubber ball in place of the iceball and a flat smooth aluminum surface in place of the ice brick. Two sets of data are presented; each symbol represents a single collision. Open circles correspond to radial impacts with the torsion pendulum fixed and unable to oscillate. Solid circles correspond to radial impacts with the torsion pendulum free to oscillate.

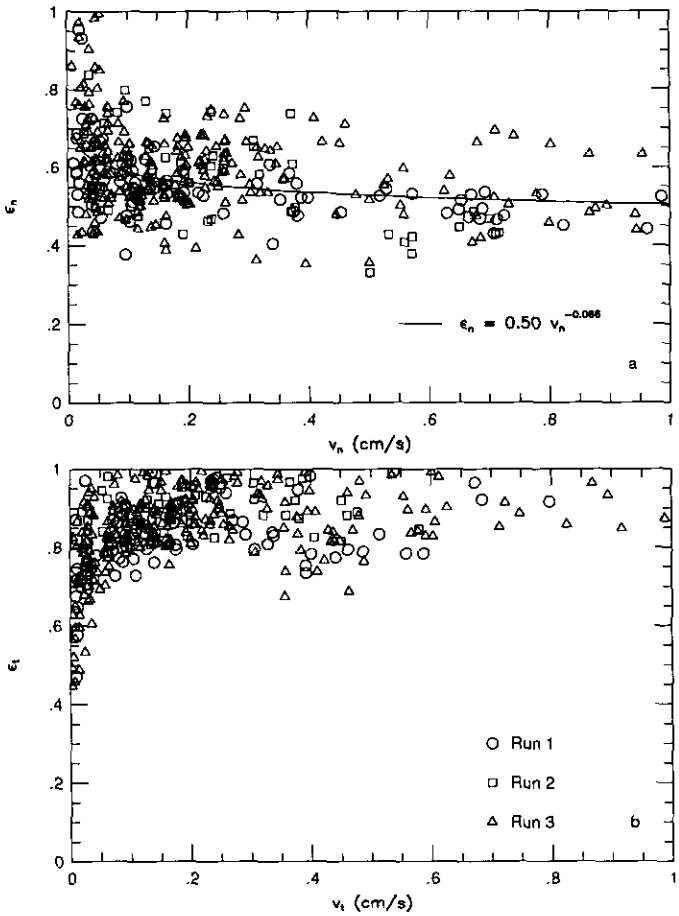

FIG. 5. Glancing collisions, smooth ice surfaces. Each symbol represents a single collision; the three different symbols correspond to three different runs with different sets of ice surfaces. The top graph shows the dependence of the normal component of ε, ε_n, on the normal impact velocity, v_n. The solid curve is a least-squares fit to the data. The bottom graph shows the dependence of the tangential component of ε, ε_t, on the tangential impact velocity, v_t.

tainly contributes to the uncertainty in the iceball results reported in this paper. However, the effect of these undamped motions is much smaller than the effect of the small-scale roughness of the ice surfaces themselves; the scatter in the data reported in Fig. 5, for example, is much larger than 3%.

B. Glancing Collisions

Measurements of the components of ε as a function of impact velocity for glancing collisions are shown in Fig. 5. The three different symbols in the figure correspond to three different experimental runs, each with different ice surfaces. There is a large amount of scatter in ε_n, the vertical component of ε, especially at the lower speeds (Fig. 5a). The value of ε_n decreases with increasing (normal) impact velocity over the range investigated, attaining a value of $\simeq 0.5$ at the higher speeds. A least-squares fit to all the data yields the following power law:

$$\varepsilon_n = (0.50 \pm 0.009) v_n^{-0.066 \pm 0.008}. \quad (4)$$

The velocity dependence of ε_n for these glancing collisions is even weaker than that for radial collisions with a free torsion pendulum. To emphasize this decreased dependence on v_n, we compare the fits for the data obtained in Figs. 3 and 5 in Fig. 6. For velocities ranging from $\simeq 0.05$ to 0.5 cm sec^{-1}, ε_n is depressed when the collisions occur randomly on different parts of the ice brick surface. For the glancing collisions, the horizontal motion is much larger than for the radial collisions. This suggests that for surfaces that are continually changing, ε_n may be nearly constant except at very low speeds. If one disregards the lower-speed ($v_n < 0.1$ cm sec^{-1}) collisions (i.e., those for which the results are most significantly affected by the local roughness of the surfaces), a linear least-squares fit results in the following equation:

$$\varepsilon_n = (0.59 \pm 0.009) + (-0.11 \pm 0.02) v_n. \quad (5)$$

The value of ε_n does decrease slowly with v_n at the higher speeds. The angle at which the collision occurs seems to have no significant effect on the value of ε_n, although the range of angles that can be investigated at a given normal impact velocity is restricted. We cannot, for example, perform collisions with even moderately high normal im-

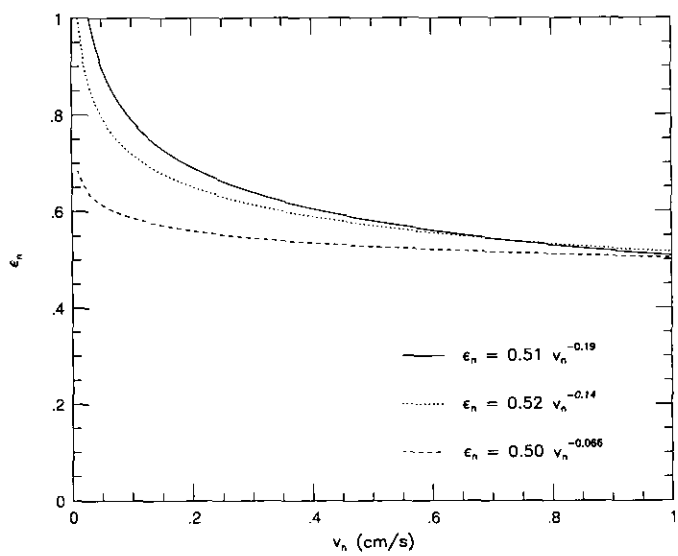

FIG. 6. Least-squares fits from Figs. 3 and 5, showing the effect of ice surface conditions on $\varepsilon_n(v_n)$ (see text). The solid line represents radial collisions with a fixed torsion pendulum. The dotted line represents radial collisions with a free torsion pendulum. The dashed line represents glancing collisions.

pact velocity (e.g., 0.3 cm/sec) and small impact angle (e.g., 10°), since this would require a large horizontal impact velocity (1.7 cm/sec), larger than we can attain with our apparatus.

The horizontal component, ε_t, shows some scatter as well, with ε_t attaining a constant value of $\simeq 0.9$ for the highest speeds (Fig. 5b). The value of ε_t, in contrast to ε_n, appears to increase with increasing v_t; however, if one again disregards the lower-speed ($v_n < 0.1$ cm sec^{-1}) collisions, ε_t behaves as follows:

$$\varepsilon_t = (0.88 \pm 0.008) + (-0.0038 \pm 0.024)v_t. \quad (6)$$

For impacts at speeds high enough to compact the ice surfaces, ε_t is constant within the scatter in the data. We were not able to investigate near-normal collisions at moderately high tangential impact velocities, because such collisions would require excessively high normal impact velocities.

The value of ε_t is consistently high, between 0.7 and 1.0 for horizontal impact speeds between 0.1 and 1.0 cm/sec, which indicates that the coefficient of friction is small. At the higher speeds appropriate to the relative motion of particles in the early outer solar nebula, ε_t approaches a constant value of $\simeq 0.9$, as discussed above. The value of ε_n is always lower, roughly 0.5 at higher normal impact speeds. In all cases there is considerable scatter that must arise predominantly from variations in the structure of the ice surfaces. For the glancing collisions, the point of contact (with an impact area $<10^{-2}$ cm^2) on the ice brick varies over a region ~ 1 cm^2 because of the slightly different periods and different starting positions of the two penduli. Thus, after many collisions, the contact surface remains only partially compacted. As discussed above for the normal collisions, the irregularities have the largest effect at the lowest speeds.

Figure 7 shows the dependence of the mass-weighted ε on impact angle θ for the data in Fig. 5. The value of ε clearly decreases with θ, from $\simeq 0.95$ for $\theta < 10°$ to $\simeq 0.55$ for $\theta > 80°$. A linear least-squares fit to the data yields the following equation:

$$\varepsilon = (1.04 \pm 0.006) + (-0.0055 \pm 0.0001)\theta. \quad (7)$$

For these smooth ice surfaces, the more glancing the collision, the smaller the energy loss. The three different symbols in the figure represent the three different runs with three different sets of ice surfaces. The datasets are consistent with one another, thus demonstrating the reproducibility of our results. The data in Fig. 7 represent the entire velocity range that we investigated; at a given angle, the total impact velocity can range from ~ 0.01 to 1.0 cm sec^{-1}.

Figure 8 shows the dependence of ε on total impact speed and impact angle for a subset of the complete dataset in Fig. 7. The complete dataset shows a continuous increase in ε as θ decreases at all impact speeds. The three ranges of θ displayed in Fig. 8 emphasize this strong dependence. These data clearly show that, for smooth

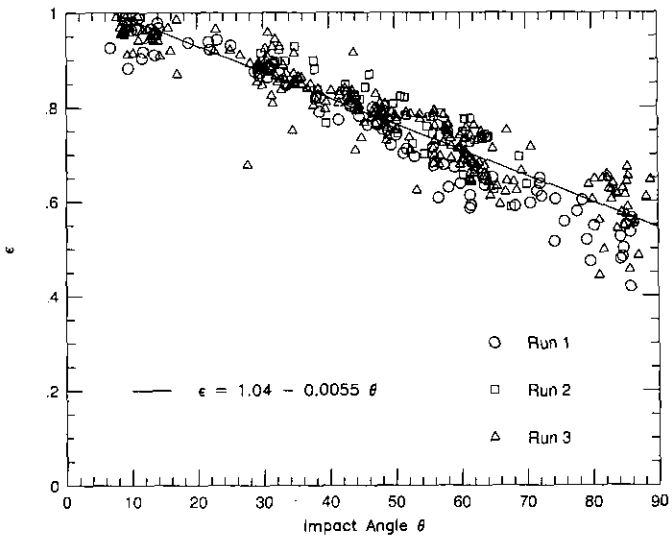

FIG. 7. The same data presented in Fig. 5, showing the dependence of the total mass-weighted coefficient of restitution, ε, on the impact angle, θ. Each symbol represents a single collision; the three different symbols correspond to three different runs with different sets of ice surfaces. The solid line is a least-squares fit to the data. The data displayed are a compilation of impacts at several different total impact speeds, ranging from 0.03 to 1.3 cm sec^{-1}.

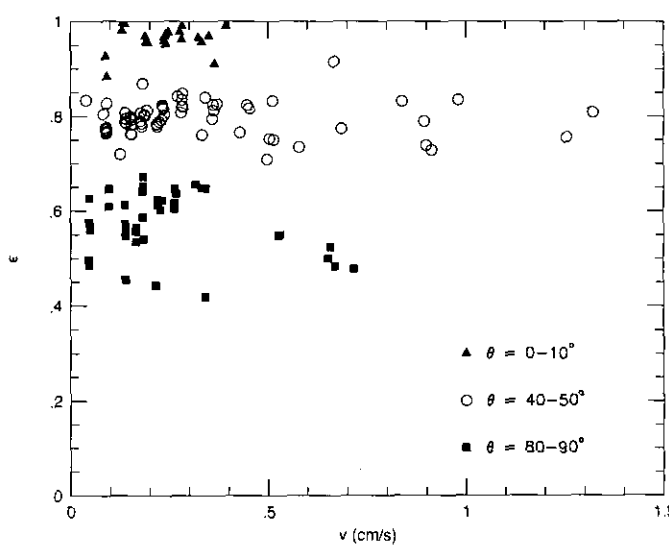

FIG. 8. The same data presented in Fig. 5, showing the dependence of the total mass-weighted coefficient of restitution, ε, on impact angle θ and total impact velocity v. Each symbol represents a single collision; the three different symbols correspond to three different ranges of impact angle, as noted in the figure.

centimeter-sized ice particles, the energy loss is significantly greater in near-normal collisions than in near-grazing collisions. For near-normal collisions (θ = 80°–90°), ε decreases slowly with v:

$$\varepsilon = (0.60 \pm 0.02) + (-0.096 \pm 0.06)v. \quad (8)$$

This equation is very similar to that calculated for ε_n vs v_n for the higher-speed collisions discussed previously (Eq. (5)). In contrast to Fig. 3, these near-normal collisions do not result in high values of ε_n at low values of v_n. (Also note that the high values of ε_n (>0.8) for $v_n <$ 0.05 cm sec^{-1} in Fig. 5 were collisions in which $\theta < 60°$.) The low-speed near-normal collisions were performed concurrently with high-speed collisions at glancing angles, which likely produced many small ice chips and fractured the brick surface over an area of ~1 cm^2. As discussed previously, the iceball does not have enough energy to compact chips on the brick surface in low-speed collisions; therefore, the resulting value of ε_n is expected to be low. The data in Fig. 8 are probably more indicative of the true nature of low-speed near-normal collisions between centimeter-sized solid icy particles in planetary rings or planetesimal disks, since those particles undoubtedly have rough, uneven surfaces. For near-grazing collisions (θ = 0°–10°), ε is constant within the scatter at 0.95; there is very little energy lost in near-grazing collisions. For intermediate θ, ε is again constant at 0.80, within the scatter. Since the iceball is not permitted to rotate upon collision, these values of ε can be regarded as upper limits.

The data in Fig. 9 were obtained at room temperature with a rubber ball in place of the iceball and a flat, sandpaper-covered aluminum surface in place of the ice brick. In contrast to Fig. 7 (the analogous iceball data), the rubber ball data show a clear minimum in the mass-weighted value of ε for 45° < θ < 60°. This minimum occurs because there is significant friction between the rubber ball and sandpaper surfaces upon collision; ε_t falls between 0.6 and 1.0 for the majority of collisions (Fig. 10b) and decreases with increasing impact angle. Notice also the high value of ε_n for the rubber ball collisions (Fig. 10a); ε_n never dips below 0.8. By performing linear least-squares fits to these data, we have determined that the value of ε_n is constant for a given range of θ, and indeed is constant at 0.93 over all θ and v_n, within the scatter in the data. In contrast, ε_t shows a clear dependence on θ. At a given v_t, the normal compressive force is larger at high impact angles than at smaller impact angles. The frictional force between the two surfaces will therefore be larger for high impact angles, and ε_t will be correspondingly lower, as shown in Fig. 10b. The iceball data for ε_t in Fig. 5b, when binned with respect to impact angle, show this same behavior, although the trend is not nearly as well-defined, since ε_t is consistently high for those

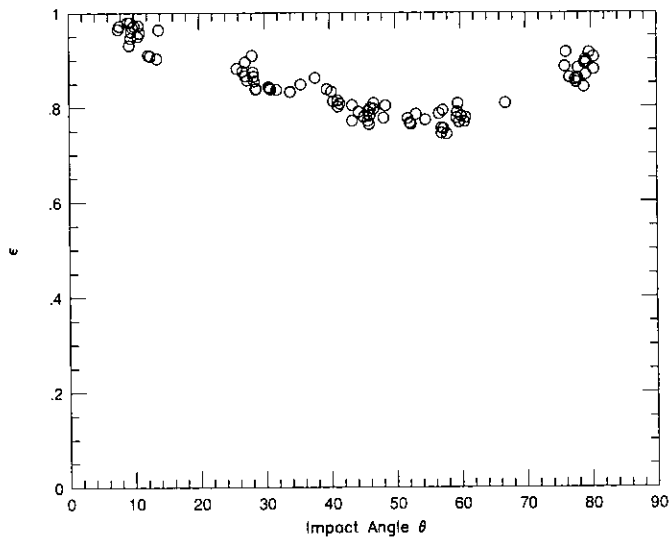

FIG. 9. Glancing collisions. These data were taken with a rubber ball in place of the iceball and a flat, sandpaper-covered aluminum surface in place of the ice brick. Each symbol represents a single collision. Note the minimum in ε as a function of impact angle θ. The value of ε has been weighted according to the effective masses of the two penduli. The data displayed are a compilation of impacts at several different total impact speeds, ranging from 0.05 to 0.7 cm sec^{-1}.

collisions (the ice surfaces were relatively smooth). For the rubber ball collisions, the combination of consistently high ε_n and decreasing ε_t with increasing θ results in the minimum in ε vs θ shown in Fig. 9.

Johnson (1983) performed rubber ball experiments similar to those reported in this paper. However, in contrast to our experiment, in which the ball is attached to a pendulum apparatus and is constrained from rotating, Johnson launched a ball freely through the air with a certain degree of backspin. The ball then impacted a hard flat surface and bounced backwards (i.e., the direction of tangential impact velocity was reversed in the collision). His data compare reasonably well with the elastic theory of Maw *et al.* (1976).

Stronge (1994) has developed a theoretical model for the oblique impact of rough compliant bodies upon a hard planar surface. For the case of a spherical body with material characteristics similar to those of a rubber ball, he finds that, for near-normal to intermediate angles of incidence, the tangential component of the incident velocity should reverse direction upon impact due to the effects of tangential compliance, even if the ball is not initially rotating. A crucial element of Stronge's theory is that the ball sticks to the surface briefly during both near-normal and intermediate-angle collisions. Our experimental apparatus appears to be well-suited to test this theory, as the rubber ball is unable to rotate. However, at the low speeds in our experiment, plastic deformation is not significant,

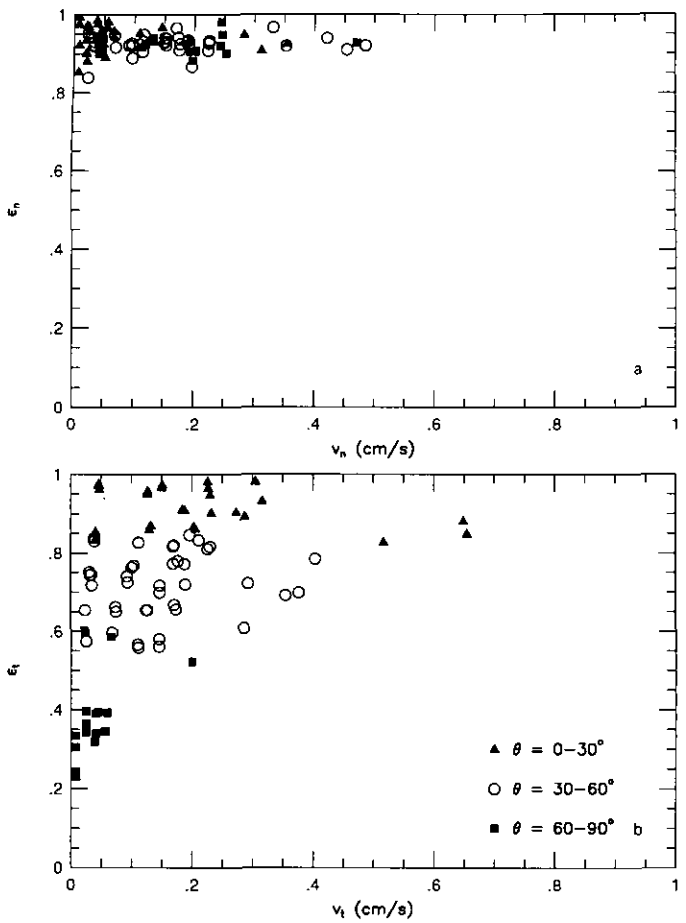

FIG. 10. The same data presented in Fig. 9, showing the dependence of the normal component of ε, ε_n, on the normal impact velocity, v_n, and the dependence of the tangential component of ε, ε_t, on the tangential impact velocity, v_t. Each symbol represents a single collision; the three different symbols represent three different ranges of impact angle, as noted in the figure.

while in the theory, it plays a major role. We do not observe tangential velocity reversals, even at near-normal impact angles (up to ≈89°). (Above 89°, the results become sensitive to the tilt of the aluminum brick, as discussed in Section II.) Since the magnitude of tangential displacement during the collision is very small (typically <50 μm, less than the size of the grains in the sandpaper on the aluminum brick), the ball most likely does not stick upon impact, as assumed in Stronge's theory. Our results indicate that, at these low speeds, tangential compliance alone will not cause a rubber ball to bounce backwards; as Johnson's work suggests, it appears that some degree of backspin is necessary. However, the moment of inertia of our torsion pendulum is a few times that of the disk pendulum, and this will make it even more difficult to achieve stick at very low tangential velocities and thus more difficult to achieve tangential velocity reversal. For the case of iceball collisions, we would not expect (and do not observe) such reversals at any impact angle, because: (1) the ball is unable to rotate, (2) the coefficient of friction is very low, (3) tangential compliance is negligible, and (4) the energy of impact is more likely to be absorbed in breaking off protrusions on the ice surfaces than in actual deformation of the ice masses themselves.

Significant friction is not present in collisions between two smooth ice surfaces, as evidenced by the consistently high value of ε_t for iceball collisions (0.8 to 1.0 for the vast majority of collisions; see Fig. 5b). We expect that collisions between two roughened (not frosted) ice surfaces will show a minimum in ε vs θ similar to that of Fig. 9, due to the increased friction. We also expect that such collisions will result in a constant (but small) $\varepsilon_n(v_n)$ and a clear dependence of ε_t on θ, as demonstrated for the rubber ball collisions in Fig. 10. The fact that the surfaces are rough will complicate the experiment, however; as discussed previously, when the two surfaces are not smooth, transfer of energy can easily take place between the disk and torsion penduli upon collision, especially at low impact speeds. We now have a measure of this energy transfer for the case of (nearly) smooth ice surfaces, and we will be able to apply this knowledge to our future investigation of the properties of rough ice surfaces.

IV. DISCUSSION

A. Interpretation of the Data

The structure of the two ice surfaces is critical in determining the value of ε. Surface irregularities include frost chips on one or both surfaces and small-scale (<100 μm) ridges, protrusions, or troughs on the ice brick. Typically, in our experiments, the iceball surface is initially completely smooth at the 10-μm level since the iceballs are made in a mold with a smooth aluminum interior. The ice brick, however, is made by simply freezing water in an open container, so it is more difficult to control the characteristics of that surface; on a 200-μm scale the "flat" ice surface is clearly uneven. This microscopic roughness causes a randomness in the collisions, both in the direction the particles separate and in the amount of energy lost in a particular collision. The effect of the randomness is largest at the lower speeds; we attribute this to the fact that there may not be sufficient impact force to fracture the contacting surfaces.

Surprisingly, there is very little frictional loss for tangential motion. Since the iceball cannot rotate, our measurements give the largest amount of loss possible for the horizontal component. The very low frictional loss observed indicates that in low-speed collisions of relatively smooth ice particles, there may be very little transfer of translational kinetic energy into rotational motion.

This result is in contrast to some collisional models and the experimental collisions of small dust aggregates at much higher speeds (Blum and Münch 1993). At some speed the impulse must become large enough that the surfaces of the two particles become locked together (no sliding) for the duration of the collision. Our measurements suggest that at the very low relative speeds expected in Saturn's rings and in some phases of the early solar nebula, relatively smooth icy surfaces will not interlock. Surface frost provides a mechanism for increased energy loss in normal collisions of icy particles (Hatzes *et al.* 1991); it is likely that frost will increase the energy loss for transverse motion as well.

B. Applications to Planetesimal Formation

Ultimately, one would like to formulate analytic expressions for $\varepsilon_n(v_n)$ and $\varepsilon_t(v_t)$ for ice particles so that the dynamics of such particles in the outer solar nebula could be modeled accurately. In the most general sense, one would like to know whether ε increases or decreases with impact velocity. From Figs. 7 and 8, it is clear that the impact angle is of greater importance in determining the energy loss in collisions than the total impact velocity, at least for the case of homogeneous, smooth ice particles. Previous work (Bridges *et al.* 1984; Hatzes *et al.* 1988) has shown that, in radial collisions, ε_n decreases with increasing impact velocity v_n over the range 0–2 cm/sec, and we have confirmed this behavior with our current apparatus over the range 0–1 cm/sec (Fig. 3). A decreasing $\varepsilon(v)$ would tend to stabilize a system of orbiting particles, keeping their relative velocities from becoming too large by dissipating more energy in deformation of the particles when relative velocities increase. Our results suggest (Fig. 8) that ε is nearly constant with v, except in the case of near-normal collisions ($\theta = 80°$–$90°$), for which ε decreases slowly with v (Eq. (8)). This behavior is a direct consequence of the absence of significant tangential friction in collisions between particles with smooth ice surfaces. The presence of chips and/or frost on one or both ice surfaces introduces a large amount of scatter into our results, especially at low speeds (<0.1 cm/sec). In fact this randomness probably must be an ingredient of any collisional model for particle dynamics, since real surfaces are expected to be irregular. At higher speeds ($\simeq$1.0 cm/sec) more relevant to particles in the solar nebula, however, ε_n and ε_t both appear to approach constant values (roughly 0.5 and 0.9, respectively). These parameter values mean that there is a large variation in the total energy loss for different angles of incidence (Fig. 7). In the opaque regions of planetary rings, differential Keplerian rotation is the main contributor to the velocity dispersion, so glancing collisions are more likely to occur. In this case, the total energy loss may be less than originally estimated.

Shu *et al.* (1985) discussed the viscous damping of nonlinear spiral density waves in Saturn's rings, in particular the density waves in the A ring created in a 5 : 3 resonance with Mimas. They determined that the observational data were fit well by postulating that the ring was made up of smooth crystalline ice particles like those used in our experiment. Shu *et al.* used the result of Bridges *et al.* (1984) for $\varepsilon_n(v_n)$ ($\varepsilon_n = 0.32 v_n^{-0.23}$) and assumed that $\varepsilon_t = 1$ (i.e., no tangential friction) in their models. Our new data indicate that there is indeed little tangential friction in collisions between two smooth ice particles. We have also confirmed the result of Bridges *et al.* for the general dependence of ε_n on v_n for purely radial collisions; however, our new data also indicate that, for surfaces which are continually changing, ε_n is nearly constant at higher impact speeds.

Araki (1988) examined the effect of spin degrees of freedom on the dynamics of a dense particle disk. He assumed that ε_n and ε_t were independent of relative impact velocity. This assumption is consistent with our results for ε_t, if one considers all but the lowest impact speeds (<0.1 cm sec^{-1}); however, ε_n does appear to decrease (slowly) with relative impact velocity. He found that if $\varepsilon_t = 1$, the translational random kinetic energy of the particles completely dominates the spin kinetic energy, while if $\varepsilon_t = -1$, there is equipartition between translational and spin energies. We have never observed $\varepsilon_t < 0$ in our experiments; in fact, ε_t is quite high, averaging $\simeq$0.9 for most collisions we performed. For a disk composed of these smooth ice particles, then, the spin kinetic energies of the particles could be very low.

The problem of particle aggregation in Saturn's rings has been examined recently by Salo (1992) and Richardson (1994). Numerical modeling of ring particle dynamics shows that gravitational wakes form in both the A and B rings; such wakes may explain observed local variations in the particle distribution in the rings. Both authors use the experimental results of Bridges *et al.* (1984) for $\varepsilon_n(v_n)$ and adopt varying degrees of surface friction (i.e., various values of ε_t). Our new data would not likely affect the general result of wake formation, as these structures appear to form under a variety of reasonable assumptions about the elastic properties of ice particles.

Hänninen and Salo (1992) have investigated the effects of a perturbing satellite on the collisional dynamics of ring particles in Lindblad resonances. They do not consider the self-gravity of the ring particles, but concentrate on their collisional properties. The particles are identical, spherical, and frictionless, and energy loss in collisions occurs only in the direction normal to the tangent plane of the impact. The coefficient of restitution is assumed to be constant with impact velocity ($\varepsilon_n = 0.1$ for most of the simulations). Again, the assumption of zero tangential friction ($\varepsilon_t = 1$) approximates the behavior of our smooth,

spherical iceballs. The value $\varepsilon_n = 0.1$, however, is likely too low. In simulations with higher $\varepsilon_n = 0.5$, Hänninen and Salo find a damping of satellite-generated ring particle orbital eccentricities due to the increased velocity dispersion of the ring particles; this case is probably more realistic, at least for smooth icy ring particles.

Ohtsuki (1993) has examined the effect of the coefficient of restitution on the capture probability of colliding bodies orbiting a central mass. In the case of collisions between equal-mass (10^{18} g) planetesimals for which self-gravity is a determining factor (note that for the centimeter-sized particles used in our work, self-gravity is not relevant), Ohtsuki estimates that as long as $\varepsilon < \varepsilon_{crit}$ ($\varepsilon_{crit} \simeq 0.8$, depending on the exact conditions involved), most collisions will lead to accretion. The capture probability falls off quite fast with increasing ε above ε_{crit}. The value of ε for these planetesimals is clearly very important in determining their dynamics; if $\varepsilon > \varepsilon_{crit}$, most collisions will not lead to capture, due to the lack of kinetic energy dissipation in collisions, and timescales for aggregation will be long. If $\varepsilon < \varepsilon_{crit}$, then timescales will be correspondingly shorter. Near the critical value of 0.8, a small change in ε can cause a large change in the overall dynamics of the orbiting particle disk.

V. CONCLUSIONS

We have measured ε for a range of glancing angle collisions and shown that the energy loss for tangential motion is much lower than for normal impacts. Our measurements indicate that for relatively smooth ice surfaces the frictional forces during contact are surprisingly small; consequently, at very low normal impact speeds there may be little transfer of translational kinetic energy into rotational motion.

These results for glancing collisions of ice particles suggest that the average value of ε in collisions may be somewhat higher than the values determined earlier in purely radial collisions, due to the high value of ε_t. In addition, the velocity dependence of ε is much weaker for the glancing collisions.

The surface characteristics of iceball and ice brick are very important to the analysis of data from this experiment. Care must be taken to account for such effects as those described above when extracting meaningful results from the measurements. Our results clearly show that tiny surface irregularities produce a large randomness in the subsequent motion of the ice particles. Such irregularities also reduce the dependence of ε_n on v_n; ε_n is nearly constant at normal impact speeds approaching 1.0 cm sec^{-1}. It is of course very likely that icy planetary ring particles or particles in the solar nebula will have surfaces which are not completely smooth; in that case, our data could be applicable to centimeter-sized icy particles in such environments. Our future experiments with macroscopically roughened ice particles will provide even more insight into the dynamics of such particles. It has been suggested (e.g., Donn and Meakin 1989, Weidenschilling and Cuzzi 1993) that centimeter-sized nebular particles were low-density aggregates of smaller particles rather than solid, unit-density bodies like the spherical iceballs we have used in our experiments. Our results for solid particles could then be useful as an upper limit to the value of ε in collisions between more porous centimeter-sized aggregates.

ACKNOWLEDGMENTS

The authors acknowledge the efforts of D. Darknell in creating the computer software to take the data reported in this paper and the work of B. Benson in helping to develop the two-dimensional pendulum. We also acknowledge the helpful critical review of an anonymous referee. This work was supported in part by NASA Grant NAGW 590 and NSF Grant AST 89-14173.

REFERENCES

AARSETH, S. J., D. N. C. LIN, AND P. L. PALMER 1993. Evolution of planetesimals. II. Numerical simulations. *Astrophys. J.* **403,** 351–376.

ARAKI, S. 1988. The dynamics of particle disks. II. Effects of spin degrees of freedom. *Icarus* **76,** 182–198.

ARAKI, S., AND S. TREMAINE 1986. The dynamics of dense particle disks. *Icarus* **65,** 83–109.

BLUM, J., AND M. MÜNCH 1993. Experimental investigations on aggregate–aggregate collisions in the early solar nebula. *Icarus* **106,** 151–167.

BRAHIC, A. 1977. System of colliding bodies in a gravitational field. I. Numerical simulations of the standard model. *Astron. Astrophys.* **54,** 895–907.

BRIDGES, F. G., A. P. HATZES, AND D. N. C. LIN 1984. Structure, stability, and evolution of Saturn's rings. *Nature* **309,** 333–335.

BRIDGES, F. G., K. D. SUPULVER, AND D. N. C. LIN 1994. In preparation.

CUZZI, J. N., J. J. LISSAUER, L. W. ESPOSITO, J. B. HOLBERG, E. A. MAROUF, G. L. TYLER, AND A. BOISCHOT 1984. Saturn's rings: Properties and processes. In *Planetary Rings* (R. Greenberg and A. Brahic, Eds.), pp. 73–199. Univ. of Arizona Press, Tucson.

DONN, B., AND P. MEAKIN 1989. Collisions of macroscopic fluffy aggregates in the primordial solar nebula and the formation of planetesimals. In *Proc. 19th Lunar Planet. Sci. Conf.*, pp. 577–580. Lunar and Planetary Institute, Houston.

GOLDREICH, P., AND S. TREMAINE 1978. The velocity dispersion in Saturn's ring. *Icarus* **34,** 227–239.

GOLDREICH, P., AND S. TREMAINE 1982. The dynamics of planetary rings. *Annu. Rev. Astron. Astrophys.* **20,** 249–284.

HÄMEEN-ANTILLA, K. A. 1982. Saturn's rings and bimodality of Keplerian systems. *Moon Planets* **26,** 171–196.

HÄNNINEN, J., AND H. SALO 1992. Collisional simulations of satellite Lindblad resonances. *Icarus* **97,** 228–247.

HATZES, A. P., F. G. BRIDGES, D. N. C. LIN, AND S. SACHTJEN 1991. Coagulation of particles in Saturn's rings: Measurements of the cohesive force of water frost. *Icarus* **89,** 113–121.

HATZES, A. P., F. G. BRIDGES, AND D. N. C. LIN 1988. Collisional

properties of ice spheres at low impact velocities. *Mon. Not. R. Acad. Sci.* **231,** 1091–1115.

JOHNSON, K. L. 1983. The bounce of "superball." *Int. J. Mech. Eng. Ed.* **111,** 57–63.

LIN, D. N. C., S. J. AARSETH, AND P. L. PALMER 1993. Submitted for publication.

LIN, D. N. C., AND P. H. BODENHEIMER 1981. On the stability of Saturn's rings. *Astrophys. J. Lett.* **248,** L83–L86.

LIN, D. N. C., AND J. C. B. PAPALOIZOU 1980. On the structure and evolution of the primordial solar nebula. *Mon. Not. R. Acad. Sci.* **191,** 37–48.

LIN, D. N. C., AND J. C. B. PAPALOIZOU 1985. On the dynamical origin of the solar system. In *Protostars and Planets II* (D. Black and M. Matthews, Eds.), pp. 981–1072. Univ. of Arizona Press, Tucson.

LUKKARI, J. 1981. Collisional amplification of density fluctuations in Saturn's rings. *Nature* **292,** 433–435.

MAW, N., BARBER, J. R., AND FAWCETT, J. N. 1976. The oblique impact of elastic spheres. *Wear* **38,** 101.

MIZUNO, H., W. MARKIEWICZ, AND H. VÖLK 1988. Grain growth in turbulent protoplanetary accretion disks. *Astron. Astrophys.* **195,** 183–192.

OHTSUKI, K. 1993. Capture probability of colliding planetesimals: Dynamical constraints on accretion of planets, satellites, and ring particles. *Icarus* **106,** 228–246.

PALMER, P. L., D. N. C. LIN, AND S. J. AARSETH 1993. Evolution of planetesimals. I. Dynamics: Relaxation in a thin disk. *Astrophys. J.* **403,** 336–350.

RICHARDSON, D. C. 1994. Tree code simulations of planetary rings. *Mon. Not. R. Acad. Sci.* **269,** 493–511.

SALO, H. 1992. Gravitational wakes in Saturn's rings. *Nature* **359,** 619–621.

SHU, F. H., L. DONES, J. J. LISSAUER, C. YUAN, AND J. N. CUZZI 1985. Nonlinear density waves: viscous damping. *Astrophys. J.* **299,** 542–573.

SHU, F. H., AND G. R. STEWART 1985. The collisional dynamics of particulate disks. *Icarus* **62,** 360–383.

STEWART, G., D. N. C. LIN, AND P. H. BODENHEIMER 1984. Collision-induced transport processes in planetary rings. In *Planetary Rings* (R. Greenberg and A. Brahic, Eds.), pp. 447–512. Univ. of Arizona Press, Tucson.

STRONGE, W. J. 1994. Planar impact of rough compliant bodies. *Int. J. Impact Eng.* **15,** 435–450.

VÖLK, H., F. JONES, G. MORFILL, AND S. RÖSER 1980. Collisions between grains in a turbulent gas. *Astron. Astrophys.* **85,** 316–325.

WARD, W. R. 1981. On the radial structure of Saturn's rings. *Geophys. Res. Lett.* **8,** 641–643.

WEIDENSCHILLING, S. J., AND J. N. CUZZI 1993. Formation of planetesimals in the solar nebula. In *Protostars and Planets III* (E. H. Levy and J. I. Lunine, Eds.), pp. 1031–1060. Univ. of Arizona Press, Tucson.